Diffuse optical probes of particle motion and structure formation in an electrorheological fluid

J. M. Ginder
Research Laboratory, Ford Motor Company, P.O. Box 2053, M.D. 3028, Dearborn, Michigan 48121-2053
(Received 18 December 1992)

While severe multiple scattering precludes direct observation of the spatial arrangement of the particles suspended in most electrorheological (ER) fluids, both diffuse optical transmittance and diffusing-wave spectroscopy are useful noninvasive probes of particle motion in these materials. The temporal variation of the diffuse transmittance of a commercial ER fluid provides a measure of the time scale for field-induced structure formation. The response times observed with low static fields and with alternating fields are consistent with the expected induced-dipole attraction between particles. However, the field dependence of the response times measured with high static fields suggests that monopole forces play a role in the aggregation process in this fluid. The relevance of particle charge is confirmed by a novel application of diffusing-wave spectroscopy: detection of the oscillatory electrophoretic motion of the particles induced by alternating electric fields. Possible consequences of particle charge for the behavior and performance of electrorheological fluids are discussed.

PACS number(s): 82.70.Dd, 82.45.+z, 66.90.+r

I. INTRODUCTION

Electrorheological (ER) fluids, suspensions of polarizable particles dispersed in relatively nonpolar media, may soon allow the commercialization of novel electromechanical technologies based on the reversible fluid-to-viscoelastic solid transitions that they undergo upon exposure to large (~kV/mm) electric fields [1–3]. Winslow [4], who is credited with the discovery and popularization of the ER effect over four decades ago, first recognized that both the dielectric mismatch between the suspended particles and the suspending fluid and the appearance of field-induced fibrillar structures are important in obtaining ER behavior. While potential applications of ER fluids have been explored nearly continuously since that time, both the nature of the interparticle interactions and the role of the field-induced structure persist as central scientific issues in the field [5–7].

Recent progress in describing the polarization-induced interparticle forces has included semianalytical [8,9] and numerical [10–12] approaches to treat the local-field effects and multipole moments that are important in dense suspensions; these effects can substantially enhance the field-induced interparticle attraction over that predicted from the dipole approximation alone [11]. Moreover, it has recently been appreciated that field-induced particle polarization can result not only from a dielectric mismatch between particle and suspending fluid, but also from a conductivity mismatch [8,13] that leads to particle polarization through the transport of charge carriers to or around the particle surface.

The ground-state structure of the solid formed when ER fluids are exposed to high electric fields has also attracted considerable attention recently. Within the dipole approximation, a body-centered-tetragonal (bct) lattice was found to be the minimum energy structure [14,15], while in the high-dielectric-contrast limit where the dipole approximation fails, the bct structure is degenerate with face-centered-cubic and body-centered-cubic lattices [16]. The bct structure has recently been observed in a light-scattering study of an ER fluid containing large glass spheres [17].

The mechanism by which the ER solid is formed is also of great scientific and technical interest. The kinetics of structure formation largely determines the response time of the field-induced rheological changes, an important figure of merit [18] for ER device design [19]. The most technologically important features of ER fluids, their dramatically field-dependent shear and longitudinal [20] moduli and yield stresses, are presumably also affected by the nature of the solid structure, though the role of disorder on ER rheology has not been widely studied.

Optical microscopy has been widely used to characterize the kinetics of chain formation in two-dimensional aqueous colloids undergoing electric- [21] and magnetic-field-induced [22] aggregation. In the nonaqueous media more typical of practical ER fluids, the time required to form the first percolating chain upon the application of electric fields was recently measured [18]; poor reproducibility of the percolation time values apparently reflected their sensitivity to variations in the initial arrangement of the aggregating particles. Several optical studies of chain formation and aggregation in three-dimensional systems have also been reported. Model suspensions of sterically stabilized silica particles have been used in studies of chain formation through the induced anisotropy of the suspension refractive index [23], and were utilized in a recent light-scattering study [24] that probed the kinetics of the eventual coalescence of chains into larger three-dimensional structures. In less ideal suspensions, field-induced turbidity changes have been correlated with particle alignment and chain formation [25,26].

A comparison of recent theoretical models of ER structure growth and evolution suggests that the nature of this process depends sensitively on the volume fraction of suspended particles and on the dimensionless interac-

tion strength λ, which is defined as the ratio of the dipole-dipole attraction energy between pairs of touching particles to the thermal energy. For $\lambda \lesssim 1$, no aggregation takes place. For dilute suspensions in which $\lambda \gtrsim 1$, Halsey and Toor [27] have shown that structure formation occurs in two steps: initial and effectively instantaneous chain formation, followed by the gradual coalescence of the chains into columns of particles ordered in three dimensions. By contrast, Hass's molecular-dynamics (MD) simulations [28] of dense suspensions in the $\lambda \gg 1$ limit show that the suspended particles are kinetically trapped into nonequilibrium structures that possess no obvious lateral order. Qualitatively similar structures were observed in MD simulations by Melrose [29].

It is of great importance to understand and control the structure-formation process in real three-dimensional ER fluids, particularly in light of the complex and poorly characterized interparticle interactions within them. Unfortunately, two-dimensional microscopic studies obviously involve systems of reduced dimensionality and generally sample a limited number of particles. Moreover, the deliberately simplified properties of three-dimensional model colloids may lead to interparticle interactions quite different in nature and strength than those of practical ER fluids. Given the limitations of these approaches, more generic techniques to study directly the structural properties of real ER fluids are desirable. This paper demonstrates the utility of diffuse optical probes [30]—diffuse transmittance and diffusing-wave spectroscopy—in inferring the kinetics of structure formation, the motion of the particles in dense ER suspensions, and the nature of the electrostatic interactions responsible for ER solid formation [31].

The results of a detailed study of the optical and dielectric properties of a commercial ER fluid are presented. The suspension incorporated particles whose complex refractive index differed substantially from the suspending fluid, leading to severe multiple scattering and a diffuse visual appearance typical of most practical ER fluids. The length dependence of the diffuse optical transmittance of the unelectrified fluid was consistent with that expected for an absorbing, multiply scattering material. The sensitivity of diffuse transmittance to the spatial relationship between scatterers was exploited by measuring the time-resolved increase in diffuse transmittance caused by field-induced structure formation in this suspension. In particular, the dependence of the time scale τ_s for structure formation in an applied field E_0 was inferred. For low fields, $\tau_s \propto E_0^{-2}$, consistent with the expected role of induced-dipole attractive forces between particles. The seemingly paradoxical crossover at high fields and short times to a regime in which $\tau_s \propto E_0^{-1}$ implies that structure formation is affected by another process; that the corresponding rate is linearly proportional to the applied field suggests that monopole forces play a role in particle aggregation. The relevance of particle charge was confirmed by measurements of the electrophoretic mobility in dilute suspensions as well as by the observation of particle motion in the original suspensions using diffusing-wave spectroscopy.

The contents of this paper are as follows: First, the characteristics of the ER fluid and the experimental procedures utilized to study it are described. Second, the results of the optical and electrical measurements are presented. Third, discussions on the inferred structure formation kinetics and the existence of monopole effects are incorporated. Speculation on the broader consequences of particle and counterion charge are included in the summary.

II. MATERIALS AND EXPERIMENTAL METHODS

The electrorheological fluid used in this study was obtained commercially from Advanced Fluid Systems (AFS) [32]; it consisted of particles of the hydrated lithium salt of poly(methacrylic) acid suspended at a volume fraction $\phi = 0.35$ in a chlorinated hydrocarbon oil, Cereclor 50LV from ICI. While this suspension was not stabilized against sedimentation, the sedimentation rate was low enough—on the order of mm/week—that individual measurements were not affected. Some care was taken, however, to thoroughly mix the stock suspension before undertaking new sets of measurements. The suspended particles were shaped like rather irregular polyhedra and were broadly distributed in size: an average length $\bar{L} = 2.6 \pm 0.6$ μm and width $\bar{W} = 1.9 \pm 0.5$ μm was determined from optical and electron micrographs of thin layers of diluted suspension [33]. Independent estimates of the particle size were obtained from dynamic light-scattering (DLS) [34] measurements on suspensions of the particles diluted in cyclohexane. Scattered light from a sample was collected using a Brookhaven Instruments BI-200SM goniometer-detector assembly; the time autocorrelation function of the scattered light intensity was computed by a Brookhaven Instruments BI-2030AT digital correlator. The measured correlation function decays were analyzed by the method of cumulants to obtain the average and variance of the decay time distribution. The resulting effective particle hydrodynamic diameter, 2.2 ± 0.4 μm, was in good agreement with that expected [34] for the translational diffusion of prolate ellipsoids having major and minor axes lengths given by the above values of $\bar{L}$ and $\bar{W}$. Where necessary for later analyses, the particles were modeled as spheres of diameter $2a \equiv (\bar{L}\,\bar{W}^2)^{1/3} = 2.1$ μm.

The suspending fluid was isolated by centrifugation and subsequent filtration to enable determination of several base fluid properties at room temperature, 298 ± 1 K. Using a Carri-Med controlled stress rheometer, the room-temperature viscosity was found to be $\eta_f = 0.089$ Pa s. An Abbe refractometer was used to measure a refractive index $n_f = 1.495$, while measurements of the fluid absorbance yielded an attenuation coefficient $\alpha_f = 0.11$ cm^{-1} at a wavelength $\lambda_{vac} = 488$ nm. The dielectric properties of the fluid were measured in a cell possessing stainless-steel disk electrodes attached to a Solartron 1260 impedance analyzer; the high sample impedance required that the sample current be amplified by a Keithley 427 current-to-voltage converter. The measured frequency-dependent impedance was described by a parallel resistor-capacitor circuit and was consistent with

a frequency-independent conductivity $\sigma_f = 4.6 \times 10^{-9}$ $\Omega^{-1}\,m^{-1}$ and a relative dielectric permittivity $\epsilon_f = 8.1$.

The electrophoretic mobility of the particles was determined using light-beating spectroscopy [35]. The experimental configuration followed that of Uzgiris [36]; the sample was placed in a rectangular glass cuvette and parallel platinum electrodes with separations between 1 and 2 mm were inserted. The electrodes were driven by square waves of frequency between 0.1 and 1 Hz and field amplitudes of less than 100 V/mm in order to induce electrophoretic motion. Light scattered by the moving particles was mixed with that scattered from the exit face of the cuvette; the resulting light-beating or heterodyne autocorrelation decay was detected using our DLS apparatus. Uniform particle motion produces oscillations in the autocorrelation function at a Doppler frequency proportional to the particle velocity, while a velocity variance gives rise to a Gaussian temporal decay envelope [37,38]. From these observed behaviors, the magnitude of the average mobility was found to be $|\mu| \approx 4 \times 10^{-7}$ cm^2/V s, in reasonable agreement with previous mobility measurements on a similar colloidal system [39]. The relatively large measured standard deviation of the mobility, $\sqrt{\Delta\mu^2} \approx 2.2 \times 10^{-7}$ cm^2/V s, may reflect the random distribution of orientations of these nonspherical particles [40]. Given the absence of electrode polarization phenomena in the base fluid at the frequencies used, as well as the details of the cell geometry, the electrophoresis measurements were not likely to be affected substantially by electrode polarization, conductivity effects, or other causes of electric field or particle velocity nonuniformity [41].

The diffuse transmittance of the ER fluid was measured using an arrangement shown schematically in Fig. 1 [31]. The sample was held between a pair of parallel, semitransparent conducting glass electrodes sealed by a latex rubber membrane. The front electrode was mounted on a two-axis translation stage allowing the application of shear and longitudinal stresses to the sample. The sample cell was illuminated by linearly polarized light with wavelength $\lambda_{vac} = 0.488$ μm from an argon-ion laser; the laser beam was expanded by a lens pair, then apertured to produce a collimated beam of diameter ~ 1.5 cm that impinged on the front electrode. Mounted just behind the rear electrode was an apertured silicon photodiode detector to detect a portion of the light that

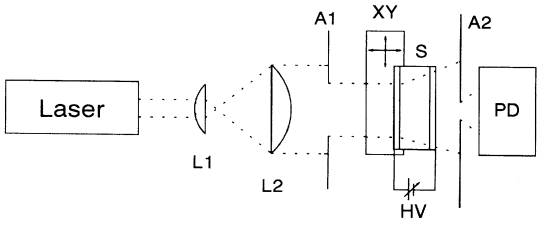

FIG. 1. Sketch of the diffuse transmittance apparatus. Laser, argon-ion laser; $L1$, $L2$, lenses; $A1$, $A2$, apertures; S, sample and transparent electrodes; XY, two-axis translation stage; HV, high-voltage amplifier; PD, silicon photodiode detector.

was diffusely transmitted through the sample; the photodetector-preamplifier bandwidth was estimated at greater than 10 kHz. High voltage was applied to the sample electrodes via a Trek 10/10 high-voltage amplifier driven by a Wavetek 75 arbitrary function generator. The temporal variation of the incident intensity, transmitted intensity, applied voltage, and current were recorded using an 8-channel, 100-kHz, 12-bit analog-to-digital converter controlled by a personal computer.

The diffuse transmittance of the sample, T, was calculated as the ratio of the intensity transmitted by the sample to the incident intensity; corrections were made for the angular variation of the photodiode response—necessary because diffusely transmitted light is spread in a nearly Lambertian distribution [42] throughout 2π solid angle—as well as for the reflectance of the electrode faces. The electric-field-induced change in T for light incident normal to the electrodes, i.e., parallel to the applied electric field $\mathbf{E}_0$, were normalized to the zero-field transmittance by calculating $\Delta T(t)/T(0) \equiv [T(t) - T(0)]/T(0)$, a measure of the transmittance change that is independent of the system geometry if the angular distribution of transmitted light was unaltered by the field-induced structural change.

Fluctuations in the speckle intensity of multiply scattered light exiting the sample were studied using diffusing-wave spectroscopy (DWS) [30,43–46]. The ER fluid was held in a cuvette into which conducting glass electrodes had been inserted; a portion of the light transmitted or reflected diffusely from the sample was imaged by a 10-cm focal length biconvex lens through a sheet polarizer onto the face of a 50-μm core diameter nonpolarization-preserving multimode optical fiber. Light exiting the opposite end of the fiber was directed to the photomultiplier tube also used in DLS measurements, allowing the measurement of intensity autocorrelation decays in the multiple-scattering regime.

III. EXPERIMENTAL RESULTS

The room-temperature dielectric response of the ER fluid mixture, Fig. 2, exhibited a more strongly frequency-dependent complex permittivity than that of the suspending fluid. The dramatic variation of ϵ' and ϵ'' as the frequency was varied is consistent with well-known double-layer polarization effects [47,48] and is in agreement with the response observed previously in similar systems [49].

The path-length dependence of the diffuse transmittance of the ER fluid, Fig. 3, was dominated by an exponential decrease with increasing sample length L. Although this exponential dependence is suggestive of the Lambert-Beer law for absorbing media, that the transmittance extrapolated to $L = 0$ is less than unity is symptomatic of multiple scattering. For $L \lesssim 0.7$ mm, the transmittance varied approximately inversely with L, as shown in the inset to Fig. 3. While the incident light was linearly polarized, the transmitted light was observed to be completely depolarized, providing additional evidence for severe multiple scattering in this material [44].

The time-resolved change in diffuse transmittance for a

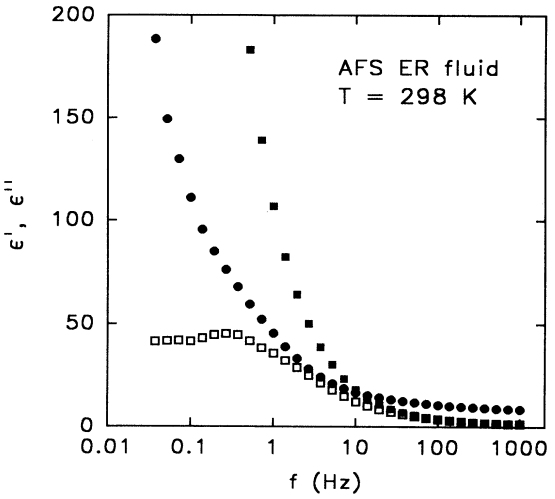

FIG. 2. Frequency dependence of the relative permittivity of the ER fluid at room temperature: ϵ' (●) and ϵ'' (■) are the real and imaginary parts of the permittivity, respectively, and $\epsilon''_{ac} \equiv \epsilon'' - \sigma(0)/\epsilon_0\omega$ (□).

sample with $L = 2.0$ mm induced by static electric fields having magnitudes ranging from 0.05 to 2.4 kV/mm is shown in Fig. 4. The $\Delta T(t)/T(0)$ initially increased upon the application of the field at time $t = 0$, then saturated at a field-dependent level of order 10%; this steady-state transmittance change persisted for tens of minutes after removing the field, though the original transmittance was regained by applying shear or normal stresses, stirring, etc., apparently destroying the residual field-induced structure. The transmittance change initially increased quadratically with time, Fig. 5, particularly at high fields.

The increase of the diffuse transmittance upon application of ac electric fields was qualitatively different; compared to the static field behavior, the response was slower and the steady-state transmittance change was smaller

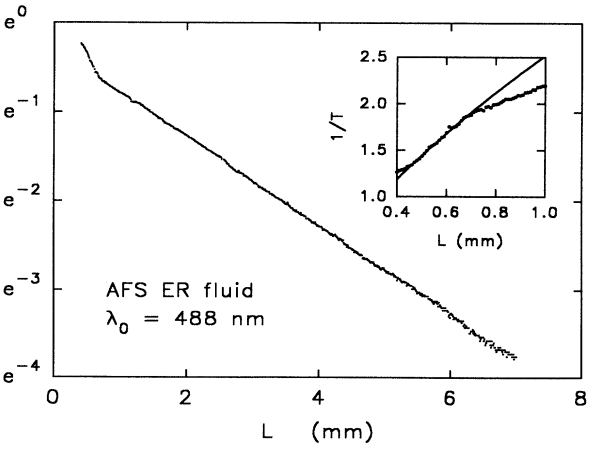

FIG. 3. Sample-length dependence of the diffuse transmittance T. Inset: the dependence of $1/T$ on L for short path lengths; the solid line is a guide to the eye.

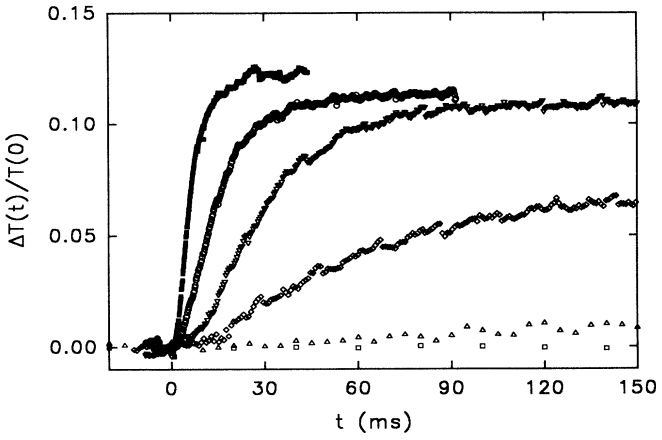

FIG. 4. The field-induced change in transmittance $\Delta T(t)/T(0)$ measured at several fields: 50 V/mm (□); 200 V/mm (△); 350 V/mm (◇); 500 V/mm (▽); 1000 V/mm (○); 2400 V/mm (■).

for, e.g., 300-Hz sine wave excitation in this system. The growth of $\Delta T/T(0)$ was fitted to a biexponential function [31], allowing the extraction of rise times and limiting transmittance changes. For ac excitation, the associated times and transmittance changes were obtained from the shorter of the two exponentials fitted to $\Delta T/T(0)$. For static fields, the characteristic response time τ_s was defined as the time required to reach $1/e$ of the steady-state transmittance change; these times and the values of the steady-state transmittance change are shown in Fig. 6. The relevant time scales decreased by over three orders of magnitude as the static field was increased from 50 to 3000 V/mm. The characteristic times varied as E_0^{-2} for low-field dc and 300-Hz ac excitation, while they were proportional to E_0^{-1} for high static fields.

Diffusing-wave spectroscopy was performed in order to gain more insight into the particle motion induced by applied electric fields. The intensity autocorrelation func-

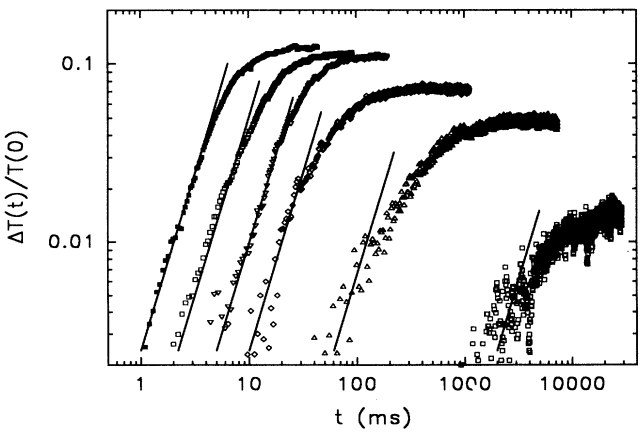

FIG. 5. Same as Fig. 4, except on a logarithmic scale. Note that $\Delta T(t)/T(0)$ grows quadratically with time at short times, as the solid lines indicate.

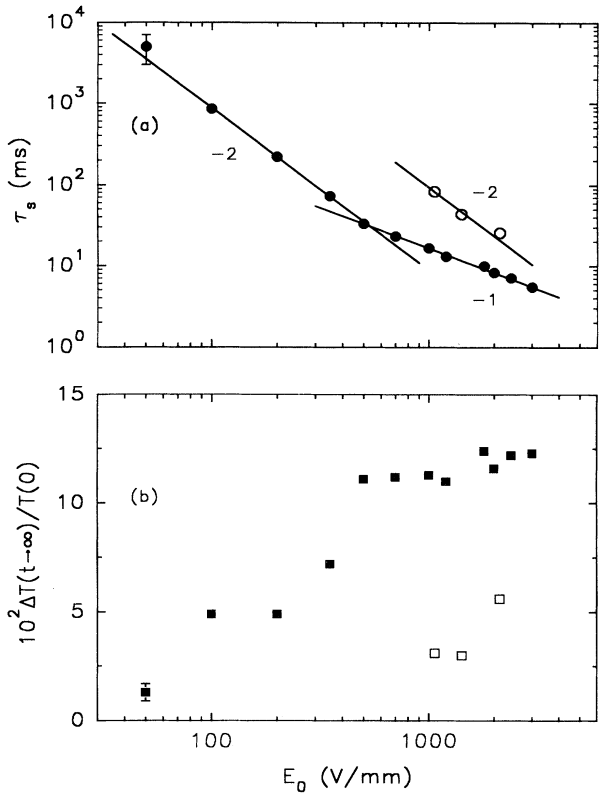

FIG. 6. Electric field dependence of (a) the inferred response time τ_s, where the power-law exponents describing the field dependences are indicated; (b) the steady-state transmittance change $\Delta T(t\to\infty)/T(0)$ for static field (solid symbols) and 300-Hz sine wave (hollow symbols) excitation.

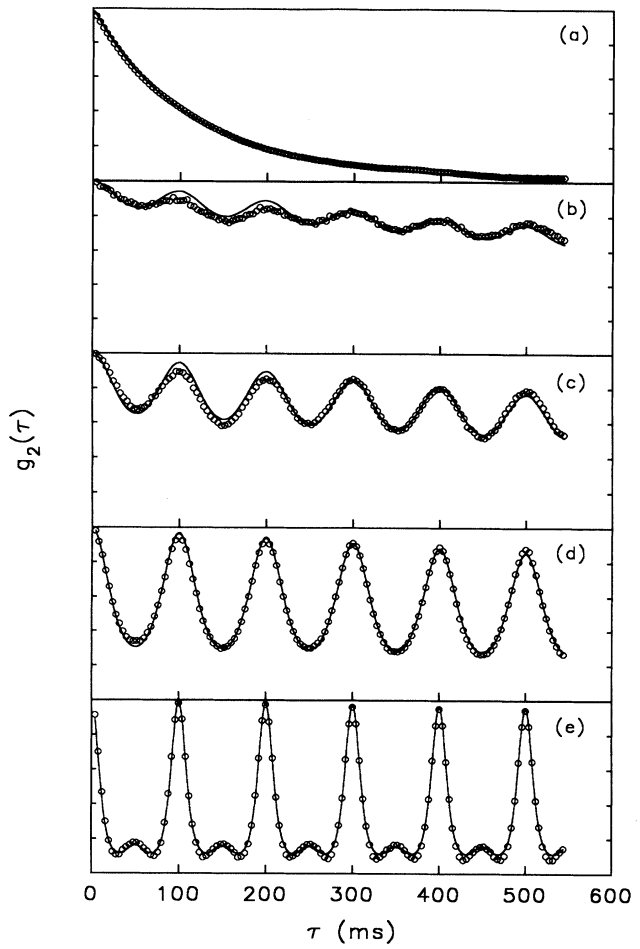

FIG. 7. The temporal evolution of the normalized homodyne autocorrelation function $g_2(\tau)$ measured in the transmission geometry for a sample of length $L=3$ mm in (a) zero field and with 10-Hz sine wave electric fields of amplitude (b) 100 V/mm, (c) 167 V/mm (d) 500 V/mm, and (e) 1000 V/mm. The range of each ordinate is $0<g_2<1$. The solid lines are least-squares fits to the autocorrelation decay predicted from Eq. (14).

tion $g_2(\tau)$ was measured in transmission with zero applied field and with 10-Hz sine wave fields of varying amplitudes, Fig. 7. Similar autocorrelation decays were observed in a backscattering geometry. To ensure that the transmitted light was multiply scattered, scattered light having polarization orthogonal to that of the incident beam was detected. The data were generally collected and averaged over 5–10 min; potential transient effects associated with the initial stages of particle aggregation were avoided. No steady-state modulation of the (angle-averaged) diffuse transmittance was observed, so the oscillations present in the measured autocorrelation functions represent speckle intensity variations produced by interference among various light paths inside the sample.

IV. DISCUSSION

The difficulties that arise in treating the multiple scattering of light in homogeneous media can be avoided in the strong-scattering limit, in which the photons execute a random walk through the sample [30,42–46,50–53]. In this limit, the spatial variation of the photon density can be described by a diffusion equation with diffusion constant $D=cl^*/3$, where c is the speed of light in the medium and l^* is the transport mean free path or average step size of the random walk. Solving the diffusion equation can be complicated by the boundary conditions: the nature of the conversion of collimated incident photons to diffusing photons [51], the consequences of reflectivity at the sample boundaries [52], etc. Two regimes of diffuse photon transport are identifiable [53]. For sample lengths L such that $l_{\rm abs}>L\gtrsim l^*$, where $l_{\rm abs}=\sqrt{l^*/3\alpha}$ is an effective absorption length for photons diffusing in a medium having an absorption coefficient α, the diffuse transmittance is given by

$$T\approx\frac{5l^*}{3L+4l^*}\ ; \tag{1}$$

the transmittance essentially varies inversely with the sample length, analogous to electronic conduction in Ohmic materials. For sample lengths $L\gtrsim l_{\rm abs}$, the diffuse transmittance is approximately

$$T \approx \frac{10l^*}{3l_{\rm abs}} \exp(-L/l_{\rm abs}) ; \quad (2)$$

the transmittance decreases exponentially with sample length, reminiscent of the Lambert-Beer law.

The measured length dependence of the diffuse transmittance, Fig. 2, exhibited both the absorptive and photon conductance regimes; a transport length $l^* \approx 450$ μm and an absorption length $l_{\rm abs} \approx 2.0$ mm was obtained from the former. The calculated absorption coefficient $\alpha \approx 0.35$ cm^{-1} at 488 nm, somewhat larger than that measured directly for the base fluid. A best fit of $T(L)$ in the latter regime to Eq. (1) yielded $l^* \approx 440$ μm, in good agreement with that obtained in the dominant absorptive regime.

Upon differentiating Eq. (2), one obtains

$$\frac{\Delta T(t)}{T(0)} \approx \frac{1}{2}\left[1+\frac{L}{l_{\rm abs}}\right]\frac{\Delta l^*(t)}{l^*(0)} . \quad (3)$$

Consequently, the increase in diffuse transmittance upon the application of an electric field is consistent with an increase in the transport length l^*; since $l_{\rm abs} \approx L = 2.0$ mm, the diffuse transmittance changes in Fig. 4 imply increases of order 10% in the transport length.

The sensitivity of the transport length l^* to the spatial arrangement of scatterers gives rise to the observed changes in diffuse transmittance, making them a useful structural probe. For identical scatterers that are spatially uncorrelated, $l^* = 1/n_p\sigma$, where n_p is the number density of scatterers and σ is the transport cross section. The transport cross section and the corresponding transport length are determined by the integral over scattering angle θ of the scattered intensity, which is proportional to the particle scattering form factor $F(q)$ [54], weighted by $1-\cos\theta$:

$$\frac{1}{l^*} \propto n_p \int_0^{2k_i} dq\, q^3 F(q) , \quad (4)$$

where $|q| = (2\pi/\lambda_0)\sin(\theta/2)$ is the magnitude of the scattering wave vector. When particle correlations are important, such as in dense or interacting suspensions, the scattered intensity for wave vector q is given by the product of the form factor and the structure factor $S(q)$, where the latter is given by

$$S(\mathbf{q}) = \frac{1}{N}\sum_{j\neq i=1}^{N}\sum_{i=1}^{N} e^{i\mathbf{q}\cdot(\mathbf{R}_j-\mathbf{R}_i)} , \quad (5)$$

where $\mathbf{R}_i$ is the position of the ith particle and N is the total number of particles. The transport length is thus determined by the structure factor through its weighted average over the scattering angle [44,45,55]:

$$\frac{1}{l^*} \propto n_p \int_0^{2k_i} dq\, q^3 F(q) S(q) , \quad (6)$$

where an isotropic $S(\mathbf{q})$ has been assumed. The sensitivity of l^* to $S(q)$ has been demonstrated repeatedly in diffuse optical studies on dense suspensions of hard-sphere colloids [44,45,55].

Existing treatments of photon transport in multiple-scattering media assume that the structure factor—and thus the transport length—is independent of the scattering direction; however, field-induced chain formation leads to a strongly anisotropic structure factor [56]. In lieu of a detailed theory relating changes in the diffuse transmittance to modifications of the structure factor, the inferred time scale for structure formation can be compared with the temporal evolution of the structure obtained in a recent three-dimensional molecular-dynamics simulation [28]. This study revealed that a characteristic time for structure formation is $\sim 10\tau_f$, where the pair-formation or flocculation time τ_f for spherical particles experiencing induced-dipole attraction and Stokes drag forces is given approximately by [28,57]

$$\tau_f = \frac{2\eta_f}{5\epsilon_0\epsilon_f\beta^2 E_0^2}\left[\left[\frac{\pi}{6\phi}\right]^{5/3}-1\right] , \quad (7)$$

where $\beta = (\epsilon_p-\epsilon_f)/(\epsilon_p+2\epsilon_f)$ is the relative polarizability of the particles. The above expression for the flocculation time is an improvement over the dilute-limit form used previously [31,57], although it was derived without inclusion of multipole and many-body electrostatic effects, which are likely to reduce τ_f, as well as many-body hydrodynamics, which would presumably increase τ_f. Within the simulation, several events characteristic of the structure formation process occur at $\sim 10\tau_f$: first, it is the stage of particle aggregation at which the average coordination number reaches 2, signaling that each particle is incorporated on average in a single chain; second, it is roughly the time at which the first percolating chain appears; third, and most relevant to the present analysis, it is an approximate rise time for field-induced changes in the structure factor.

The τ_s measured for ac and low-field dc excitation (Fig. 6) vary as E_0^{-2}, confirming that induced-dipole attractive forces are responsible for structure formation in this ER fluid. Assuming that τ_s is comparable to the characteristic structure formation time $10\tau_f$, the relative polarizability β can be estimated since the solvent viscosity and dielectric constant are known; for low static fields, $|\beta(0)|^2 \approx 0.39$, while for ac excitation a value $|\beta(300\ \text{Hz})|^2 \approx 0.037$ is inferred. The 300-Hz relative polarizability can be compared with that predicted solely on the basis of the measured complex relative permittivity of the suspending fluid, $\epsilon_f(300\ \text{Hz}) \approx 8,1+0.9i$, and of the ER fluid suspension, $\epsilon(300\ \text{Hz}) \approx 9.4+2.2i$. Utilizing the Maxwell relation [58] to describe the suspension permittivity, $\epsilon \approx \epsilon_f(1+2\beta\phi)/(1-\beta\phi)$, the squared magnitude of the relative polarizability $|\beta(300\ \text{Hz})|^2 \approx 0.041$ is estimated. While the good agreement between the polarizability inferred from the response time measurements and that obtained from the dielectric properties of the ER fluid is encouraging, other factors such as many-particle hydrodynamics and electrostatics undoubtedly influence the interparticle forces, affecting the aggregation process in poorly understood ways.

To a first approximation, the particle velocities induced by the field are determined by a balance between electrostatic and viscous drag forces. While the rate $1/\tau_s \propto E_0^2$ at low fields is thus consistent with induced-

dipole forces, that $1/\tau_s \propto E_0$ at high fields suggests that monopole forces are present, i.e., that the particles possess a nonzero surface charge. The counterintuitive crossover to a rate with a *weaker* field dependence as the field is increased is explainable by the existence of two temporally distinct aggregation processes that consequently have nonadditive rates.

To understand why such a crossover might occur, the origin of the field-induced particle polarization required for the existence of ER phenomena in this suspension must be considered. ER fluids have recently been grouped into two classes that are distinguished by differences in the way that the necessary polarization is developed [11,13,58]: those that rely on a dielectric constant mismatch between particle and fluid, and those that depend on a conductivity mismatch. While in the former systems the polarization charge appears on each particle surface almost instantaneously upon the application of an electric field, the latter rely on the transport of charge carriers—ions or electrons—to or around the interface between the particle and suspending fluid in order to develop real charge polarization and the resulting interparticle attractive forces. For systems containing spherical particles and possessing constituents with frequency-independent permittivities, the surface charge distribution is established on a time scale $\tau_p=[2\epsilon_f+\epsilon_p-\phi(\epsilon_p-\epsilon_f)]/[2\sigma_f+\sigma_p-\phi(\sigma_p-\sigma_f)]$ [59]. An approximate lower bound on τ_p is the carrier relaxation time of the suspending fluid, $\epsilon_0\epsilon_f/\sigma_f \approx 16$ ms, which is within a factor of 2 of the response time at which the crossover occurs (Fig. 6). The existence of the crossover thus suggests that for low fields, when $\tau_s \gtrsim \tau_p$, the structure evolves slowly enough to allow ion transport and thus the maximum induced-polarization forces. At high fields, no substantial particle polarization can occur when $\tau_s \lesssim \tau_p$, so that the latent surface charge largely determines the nature and strength of the electrostatic force on each particle. Implicit in this scenario is that electrophoretic motion induced by monopole–external-field or monopole-dipole interactions can promote particle aggregation; the role of such mechanisms in colloidal aggregation has not been widely explored.

The possibility that field-induced orientational alignment of the anisotropic particles in this ER fluid is the origin of the observed transmittance increase can be ruled out on a number of grounds: First, the linear dependence of the structure formation rate on electric field obtained at high fields suggests that the particles possess a permanent dipole moment, but this is not borne out by the dielectric properties of the suspension. Second, an exponential growth of $\Delta T(t)/T(0)$ is expected in light of previous studies of the field-induced orientation of ellipsoidal particles [59], while a power-law growth was observed under dc excitation. Third, the rotational time constant τ_r for the orientation of isolated particles can be estimated, $\tau_r=-\eta/[2\epsilon_f\epsilon_0 P(\beta,\bar{L}/\bar{W})E_0^2]$, where P is a function of the particle's relative polarizability and shape anisotropy [60]. Given the measured $\bar{L}/\bar{W}$ and the inferred values of β, $\tau_r/\tau_f > 3$ is obtained. Since the pair formation rate is therefore faster than the rate at which isolated particles align with the field, and since interparticle contact presumably hinders the continued rotation of individual particles, the observed changes in diffuse transmittance are not likely to be affected substantially by rotational effects.

The measured response times are also much shorter than those expected for the eventual coarsening of the field-induced chains into columns, a process that has been observed in a very different colloidal system [24]. Since the dimensionless interaction strength [5] appropriate to the particles in the AFS fluid, $\lambda=3\pi\epsilon_f\epsilon_0(\beta E_0)^2/k_BT \lesssim 10^5$ with $2a=2.1$ μm, the estimated coarsening time [24] $\tau_p \gtrsim \eta_f a^3/\lambda^{2/5}k_BT \lesssim 30$ s is orders of magnitude longer than the time scale over which the transmittance evolves at high fields.

The linear increase in the rate of aggregation with electric field in high fields suggests that the particles possess nonzero charge Q—resulting in monopole forces $\mathbf{F}=Q\mathbf{E}$—and thus undergo electrophoretic motion. Indeed, electrophoretic light-scattering experiments confirm the existence of particle charge in dilute suspensions and fix its magnitude. The effective electrophoretic mobility of charged particles depends on the concentration of counterions in suspension, or equivalently on the screening or Debye length L_D [61]. An order-of-magnitude estimate of L_D can be made after considering the dielectric response of the ER suspension, Fig. 2. The existence of a peak in the imaginary part of the dielectric response ϵ''_{ac} is consistent with models of the polarization response of the counterion cloud about charged particles in dilute suspension [47,48]. Several approaches predict a maximum in ϵ''_{ac} at a characteristic frequency ω_c dependent on the ability of the ions to diffuse around the circumference of the particle; thus $\omega_c \sim D_{\text{ion}}/2\pi a^2$, where D_{ion} is the ion diffusion constant and a is a typical particle radius. With $2a \sim 2.1$ μm and $\omega_c \sim 1$ s^{-1}, $D_{\text{ion}} \sim 3\times10^{-8}$ cm^2/s. Using the Stokes-Einstein relation, the ion mobility is estimated as $\mu_{\text{ion}} \sim eD_{\text{ion}}/k_BT \sim 1.2\times10^{-6}$ cm^2/V s; the base fluid conductivity $\sigma_{\text{ion}}=n_{\text{ion}}e\mu_{\text{ion}}$ is then consistent with a total ion density $n_{\text{ion}} \sim 2.4\times10^{14}$ cm^{-3}. The associated Debye length $L_D=(\epsilon_f\epsilon_0 k_BT/e^2 n_{\text{ion}})^{1/2} \sim 0.22$ μm is consistent with an intermediate degree of screening, $a/L_D \sim 5$ [61]. In this screening-length regime the mobility and surface or ζ potential are approximately related by the Hückel equation [61], which yields $|\zeta|=3\eta_f|\mu|/2\epsilon_0\epsilon_f \approx 63$ mV. The surface potential sets an upper bound on Q through simple electrostatics, $\zeta \gtrsim Qe/4\pi\epsilon_f\epsilon_0 a$, implying a substantial particle charge: $|Q| \lesssim 400e^-$.

It is of interest to consider the consequences of this particle charge in the highly concentrated suspensions typical of practical ER fluids. To measure the degree to which particle motion is influenced by electrophoresis in the parent fluid, diffusing-wave spectroscopy was performed under 10-Hz ac excitation, Fig. 7. DWS measures the normalized intensity autocorrelation function for multiply scattered light,

$$g_2(\tau)=\frac{\langle I(t)I(t+\tau)\rangle}{\langle I^2(t)\rangle}-1\ , \tag{8}$$

where $\langle y(t)\rangle = \lim_{T\to\infty}\int_0^T dt\, y(t)/T$ is a time average. For fields whose fluctuations obey Gaussian statistics, the intensity autocorrelation is related to the normalized field autocorrelation function $g_1(\tau)$ by the Siegert relation [34], $g_2(\tau)=|g_1(\tau)|^2$, where

$$g_1(\tau)=\frac{\langle E^*(t)E(t+\tau)\rangle}{\langle E^*(t)E(t)\rangle} . \tag{9}$$

The variation of the phase of the electric field upon suffering multiple scatterings gives rise to the sensitivity of DWS to particle motion; the magnitude and phase of the field can be written as $E^{(n)}(\tau) = |E^{(n)}(0)|\exp[-i\Phi^{(n)}(\tau)]$, where $\Phi^{(n)}=\sum_{i=1}^{n}\mathbf{q}_i\cdot\mathbf{r}_i(\tau)$, $\mathbf{q}_i$ is the ith scattering wave vector, and the sum is over a series of n scattering events. The phase change can be rewritten [46] as $\sum_{i=1}^{n}\mathbf{k}_i\cdot[\delta\mathbf{r}_{i+1}(\tau)-\delta\mathbf{r}_i(\tau)]$, where k_i is the incident wave vector of the $(i+1)$th scattering event and $\delta\mathbf{r}_i(\tau)$ is the change in position of the ith scatterer. It is relevant to consider deterministic motion of the scatterers, i.e., the oscillatory motion produced by velocities $\mathbf{v}_i(t)=\mathbf{v}_i\cos\omega t$ as expected for electrophoretic motion in ac fields. For such motion, the average contribution from paths of n scatterering events to the field autocorrelation function is

$$g_1^{(n)}=\left[1-\frac{k_0^2}{\omega^2}\langle\cos^2\theta\rangle\langle\Delta v^2\rangle(1-\cos\omega\tau)+\frac{k_0^4}{8\omega^4}\langle\cos^4\theta\rangle(\langle\Delta v^4\rangle+3\langle\Delta v^2\rangle^2)(1-\cos\omega\tau)^2+\cdots\right]^n ; \tag{10}$$

here k_0 is the magnitude of the photon wave vector in the fluid and $\langle\Delta v^2\rangle$ and $\langle\Delta v^4\rangle$ are the peak velocity variance and kurtosis, respectively. These terms are equivalent to the first two terms of a cumulant expansion of

$$g_1^{(n)}\approx e^{-2nf(\tau)} , \tag{11}$$

where the argument $f(\tau)$ is given by

$$f(\tau)\approx\frac{k_0^2}{2\omega^2}\langle\cos^2\theta\rangle\langle\Delta v^2\rangle(1-\cos\omega\tau)+\frac{k_0^4}{16\omega^4}[\langle\Delta v^2\rangle^2(4\langle\cos^2\theta\rangle^2-3\langle\cos^4\theta\rangle)-\langle\Delta v^4\rangle\langle\cos^4\theta\rangle](1-\cos\omega\tau)^2+\cdots . \tag{12}$$

The function $f(\tau)$ is directly proportional to the mean-square particle displacement in dilute suspensions [62]; for diffusive particle motion, $f(\tau)=\tau/\tau_B$, where $\tau_B=1/Dk_0^2$ is the Brownian time scale and D is the particle diffusion coefficient. For linear deterministic motion, $f(\tau)\propto\tau^2$ [46], while f is corrected by an additional component $l^*/2l_{\rm abs}$ when absorption is important [44]. These various contributions to $f(\tau)$ are additive if the diffusive and deterministic motions are uncorrelated [46]. Assuming that the contribution from paths of different orders add incoherently, the total field autocorrelation function is determined by a sum over all paths; in the limit of large n, the sum is replaced by an integral over photon paths of length $s=nl^*$ weighted by the probability $P(s)$ that each path length contributes [43]

$$g_1(\tau)=\int ds\, P(s)e^{-2sf(\tau)} , \tag{13}$$

where $P(s)$ and $g_1(\tau)$ can be obtained from the solution of the diffusion equation for the appropriate experiment geometry. For transmission through a slab of length $L\gg l^*$ illuminated by a collimated source it has been shown that [44]

$$g_1(\tau)\approx\frac{\frac{L}{l^*}\sqrt{6f(\tau)}}{\sinh\left[\frac{L}{l^*}\sqrt{6f(\tau)}\right]} . \tag{14}$$

The large oscillatory component observed in the DWS spectra—periodic *at the frequency ν of the applied field*—demonstrates unambiguously that electrophoretic motion is substantial even at moderate fields in these dense ER suspensions. Only at the highest field is a component at 2ν detected that could be interpreted as evidence of motion produced by dipole interactions, though it may simply reflect the nonzero particle velocity variance and kurtosis. It is emphasized that these DWS measurements are sensitive to *relative* motion of the scatterers [46]: if all the scatterers translated uniformly in response to the applied field, then the phase relationships of the electric fields scattered from them would be unchanged, and the autocorrelation function would not vary with time. Fits to Eq. (14) with $l^*/l_{\rm abs}\approx 0.23$ allow the field dependence of the standard deviation in peak velocity and the apparent Brownian time scale to be determined, Fig. 8, where motion along the field direction has been assumed, so that $\langle\cos^2\theta\rangle=\frac{1}{3}$ [46]. The standard deviation of the particle velocity increases linearly with electric field, consistent with an apparent standard deviation of the mobility $\sqrt{\Delta\mu_{\rm app}^2}\equiv\sqrt{\Delta v^2}/E\approx 2.3\times10^{-8}$ cm^2/V s at the lowest fields used. The extreme sensitivity of DWS to small relative motions of the particles [44] induced by electric fields is demonstrated by the peak-to-peak position standard deviation inferred from the velocity variance at 100 V/mm: $\sqrt{\Delta r^2}=\sqrt{\Delta v^2}/\omega\approx 7$ nm.

Since the velocity of the ith particle is determined by the product of its mobility and the local electric field, $\mathbf{v}_i=\mu_i\mathbf{E}(\mathbf{r}_i)$, the apparent mobility variance reflects contributions from both of these factors: $\langle\Delta\mu_{\rm app}^2\rangle \simeq\langle\Delta\mu^2\rangle+\langle\mu\rangle^2\langle\Delta E^2\rangle/E^2$. In addition to the variations of particle size, orientation, and surface charge that give rise to nonzero $\langle\Delta\mu^2\rangle$ in dilute suspensions, both

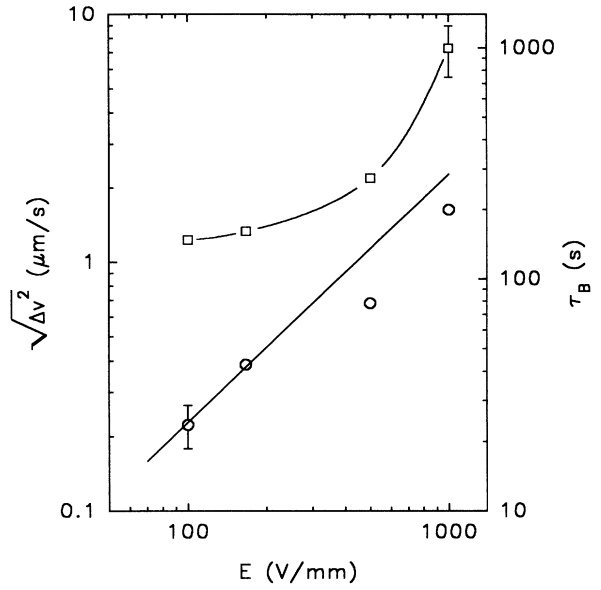

FIG. 8. Particle velocity standard deviation (○) and Brownian time scale (□) inferred from electrophoretic DWS measurements. The straight line demonstrates the roughly linear dependence of the velocity standard deviation on applied electric field; the curved line is a guide to the eye.

$\langle \Delta\mu^2 \rangle$ and $\langle \Delta E^2 \rangle$ are strongly affected by many-body interactions at high concentrations: for example, many-body hydrodynamics reduces the sedimentation rate [63] (sedimentation is the gravitational analog of electrophoretic motion) and induces a velocity variance even in suspensions of identical spheres [64]. Moreover, many-body and local-field effects produce a substantial electric field variance in dielectric composites [65]. Indeed, it is conceivable that electrophoretic DWS could be used to determine directly the local electric field variance in well-controlled colloidal systems.

That the apparent Brownian time scale τ_B increases substantially with the amplitude of the applied field (Fig. 8) demonstrates one way in which electrophoretic DWS is sensitive to ER structure formation. The increase in τ_B is qualitatively consistent with the incorporation of a field-dependent fraction of the suspended particles into a network structure, thereby reducing the number of particles undergoing diffusive motion, the effective particle diffusion coefficient, or both [66]. The dramatic increase in the apparent time scale may signal the formation of a colloidal glass [44,67]. However, that electrophoretic motion is observed even at high fields suggests that either the sample is not homogeneously rigid [69] or that the network itself translates in response to the applied field.

It has been demonstrated above that the kinetics of structure formation in ER fluids is obtained through the time scale of the diffuse transmittance increase, and that electrophoretic DWS can reveal the motion of the particles induced by alternating fields. Does the initial quadratic time dependence of $\Delta T(t)/T(0)$, Fig. 5, also contain useful information on the process of field-induced structure formation?

A reasonable starting point in addressing this issue is the time-dependent structure factor, which can be written as

$$S(\mathbf{q},t)=\frac{1}{N}\sum_{i\neq j}\sum_{i} e^{i\mathbf{q}\cdot(\mathbf{R}_i-\mathbf{R}_j)} e^{i\mathbf{q}\cdot[\mathbf{r}_i(t)-\mathbf{r}_j(t)]} , \tag{15}$$

where $\mathbf{r}_i(t)$ is the change in position of the ith particle from its zero-time position $\mathbf{R}_i$. Since each particle in a dense random suspension of uniform spheres has roughly 12 neighbors [Ref. 69] in the first coordination shell, it is reasonable to assume that $\mathbf{r}_i$ is uncorrelated with $\mathbf{R}_j$. One then has

$$\begin{aligned} S(\mathbf{q},t) &\approx S(\mathbf{q},0)\langle e^{i\mathbf{q}\cdot[\mathbf{r}_i(t)-\mathbf{r}_j(t)]}\rangle_{ij} \\ &\approx S(\mathbf{q},0)(1-\tfrac{1}{2}\langle\{\mathbf{q}\cdot[\mathbf{r}_i(t)-\mathbf{r}_j(t)]\}^2\rangle_{ij}+\cdots) , \end{aligned} \tag{16}$$

where the average $\langle \cdots \rangle_{ij}$ is over all particle pairs. Inserting Eq. (16) into the expression for the scattering length, Eq. (6), yields a relation between the increase in scattering length and the change in interparticle separation:

$$\frac{\Delta l^*(t)}{l^*(0)} \approx \frac{\int_0^{2k_i} dq\, q^3 F(q) S(q) \langle\{\mathbf{q}\cdot[\mathbf{r}_i(t)-\mathbf{r}_j(t)]\}^2\rangle_{ij}^{\Omega}}{2\int_0^{2k_i} dq\, q^3 F(q) S(q)} . \tag{17}$$

Note that uniform particle translation, $\mathbf{r}_i(t)\equiv\mathbf{r}_j(t)$, does not alter the scattering length or diffuse transmittance. The averages over scattering angle Ω and particles yield $\langle[\mathbf{q}\cdot(\mathbf{r}_i-\mathbf{r}_j)]^2\rangle_{ij}^{\Omega}=2q^2\Delta r^2(t)\langle\cos^2\theta\rangle$. Here $\Delta r^2(t)=\langle r^2(t)\rangle-\langle r(t)\rangle^2$ if the particle displacements $\mathbf{r}_i$ and $\mathbf{r}_j$ are uncorrelated, as is likely before substantial aggregation has occurred. One then obtains a scattering length change

$$\frac{\Delta l^*(t)}{l^*(0)} \approx \overline{q^2}\Delta r^2(t)\langle\cos^2\theta\rangle , \tag{18}$$

where $\overline{q^2}$ is the average of q^2 weighted by $q^3F(q)S(q,0)$.

In light of the above derivation, the quadratic increase of the diffuse transmittance with time implies that the mean-square relative particle displacement $\Delta r^2 \propto t^2$, as expected for deterministic particle motion. Such a deterministic regime has been identified from MD simulations of the early-time particle displacements [28], and is presumably a reflection of the ballistic (i.e., nondiffusive) nature of the aggregation process in ER fluids. The relationship derived between the change in scattering length and the mean-square particle displacement, Eq. (18), enables one to calculate the velocity standard deviation if $\overline{q^2}$ is known. Using Mie scattering theory for spherical particles, and assuming that the structure of the quiescent fluid is describable by the Percus-Yevick structure factor [70], upper and lower bounds on the particle refractive index $1.43\langle n_p\rangle 1.53$ produce a scattering length consistent with the measured $l^*\approx 460\ \mu$m; for particles with this range of refractive index, $\overline{q^2}\sim(0.5\pm0.04)k_0^2$. The so-inferred standard deviation in particle velocity, Fig. 9,

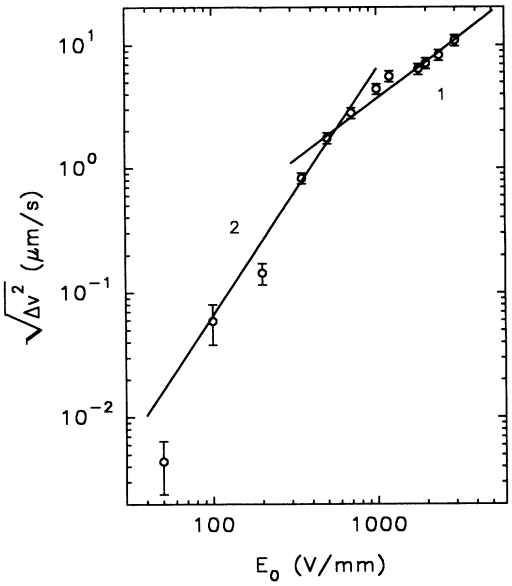

FIG. 9. Standard deviation of particle velocity inferred from the temporal dependence of the diffuse transmittance change for static fields. The power-law exponents describing the field dependences are indicated.

exhibits two regimes: at low fields, it increases quadratically with field, while at high fields, it increases linearly with an apparent mobility standard deviation $\sqrt{\Delta\mu_{app}^2} \sim 3.1\times10^{-8}$ cm^2/V s. This value is in reasonable agreement with that obtained from DWS under alternating-field excitation, suggesting that the temporal variation of $\Delta T(t)/T(0)$ does reflect the motion of the scatterers as they aggregate via electrostatic forces. Therefore, the earlier supposition that electrophoresis can promote particle aggregation at high fields is seemingly confirmed by the existence of this mobility variance.

V. CONCLUSIONS AND SUMMARY

Time-resolved diffuse optical transmittance has been used to infer the kinetics of structure formation in practical ER fluids. The commercial ER fluid under study exhibited a field-induced increase in transmittance; that the time scale for the increase varied as E^{-2} for low fields and ac excitation is completely consistent with the expected role of polarization forces in chain formation. At high fields, the time scale varied as E^{-1}, suggestive of latent monopole forces due to the inevitable surface charge on the suspended particles. The observed crossover in the field dependence of the structure formation times likely reflects the nonzero time required to form substantial dipole moments in these particles, since the polarization results from ion transport to or at the particle-solvent interface. The relevance of surface charge was confirmed by electrophoretic light scattering in dilute suspensions, as well as by electrophoretic diffusing-wave spectroscopy on the parent ER fluid. These observations provide evidence that the overall rate of structure formation can be negatively affected in "extrinsic" ER fluids [71], such as that presently studied, which rely on the transport of ions to develop a substantial ER effect. On the other hand, the results do qualitatively confirm the predictions for the characteristic structure formation time due to induced polarization forces, enabling the prediction of ER response in a wide range of materials, and showing that submillisecond responses are readily obtainable in the appropriate fluids.

The extent to which particle charge and the concomitant monopole forces affects ER phenomena is unclear. While screened Coulomb interactions are commonly used to stabilize aqueous suspensions against unwanted aggregation [61], their role in the structure formation process in ER suspensions is not obvious. The present observations suggest that monopole-external field or monopole-dipole interactions can promote some form of particle aggregation; unfortunately, models or simulations of ER fluids that include both interacting monopoles and dipoles are not available. Monopole forces might be used advantageously to densify [72] or "anneal" the imperfect structures grown by the rapid application of high fields, perhaps leading to improved rheological properties. In addition to increasing its conductivity, the requisite counterions and co-ions in the suspending will screen not only monopole but also dipole and multipole interactions, thus affecting the electrostatic energy stored in these suspensions. Thus a fruitful, albiet challenging, subject for study might be to describe the interaction of polarized double layers about pairs of particles. The associated screening length adds another length scale over which the interparticle energy varies, and thus may enhance the spatial derivatives of that energy, i.e., the elastic moduli of the induced ER solid [73].

ACKNOWLEDGMENTS

The author is grateful to Larry Elie for extensive technical assistance, to Kiel Plummer and Jagadish Sorab for their technical contributions, and to Jim Anderson, Craig Davis, Ken Hass, Irv Salmeen, and David Weitz for enlightening discussions.

[1] *Proceedings of the First International Symposium on Electrorheological Fluids,* edited by H. Conrad, A. F. Sprecher, and J. D. Carlson (North Carolina State University, Raleigh, 1989).

[2] *Proceedings of the Second International Conference on Electrorheological Fluids,* edited by J. D. Carlson, A. F. Sprecher, and H. Conrad (Technomic, Lancaster, PA, 1990).

[3] *Proceedings of the International Conference on Electrorheological Fluids: Mechanisms, Properties, Structure, Technology, and Applications,* edited by R. Tao (World Scientific, Singapore, 1992).

[4] W. Winslow, J. Appl. Phys. **20**, 1137 (1949).

[5] H. Block and J. P. Kelly, J. Phys. D **21**, 1661 (1988).

[6] A. P. Gast and C. F. Zukoski, Adv. Colloid Interface Sci. **30**, 153 (1989).
[7] T. C. Jordan and M. T. Shaw, IEEE Trans. Electr. Insul. **24**, 849 (1989).
[8] L. C. Davis, J. Appl. Phys. **72**, 1334 (1992).
[9] Y. Chen, A. F. Sprecher, and H. Conrad, J. Appl. Phys. **70**, 6796 (1991).
[10] R. T. Bonnecaze and J. F. Brady, J. Chem. Phys. **96**, 2183 (1992).
[11] L. C. Davis, Appl. Phys. Lett. **60**, 319 (1992).
[12] A. M. Kraynik, R. T. Bonnecaze, and J. F. Brady, in *Proceedings of the International Conference on Electrorheological Fluids: Mechanisms, Properties, Structure, Technology, and Applications* [3], p. 59.
[13] R. A. Anderson, in *Proceedings of the International Conference on Electrorheological Fluids: Mechanisms, Properties, Structure, Technology, and Applications* [3], p. 81.
[14] R. Tao and J. M. Sun, Phys. Rev. Lett. **67** , 398 (1991).
[15] R. Tao and J. M. Sun, Phys. Rev. A **44**, R6181 (1991).
[16] L. C. Davis, Phys. Rev. A **46**, R719 (1992).
[17] T.-J. Chen, R. N. Zitter, and R. Tao, Phys. Rev. Lett. **68**, 2555 (1992).
[18] J. C. Hill and T. H. van Steenkiste, J. Appl. Phys. **70**, 1207 (1991); J. C. Hill, N. A. Vaz, D. J. Klingenberg, and C. F. Zukoski, in *Proceedings of the International Conference on Electrorheological Fluids: Mechanisms, Properties, Structure, Technology, and Applications* [3], p. 280.
[19] D. L. Hartsock, R. F. Novak, and G. J. Chaundy, J. Rheol. **35**, 1305 (1991).
[20] J. M. Ginder (unpublished).
[21] S. Fraden, A. J. Hurd, and R. B. Meyer, Phys. Rev. Lett. **63**, 2373 (1989).
[22] G. Helgeson, A. T. Skeltorp, P. M. Mors, R. Botet, and R. Jullien, Phys. Rev. Lett. **61**, 1736 (1988).
[23] K. L. Smith and G. G. Fuller, in *Proceedings of the First International Symposium on Electrorheological Fluids* [1], p. 27.
[24] J. E. Martin, J. Odinek, and T. C. Halsey, Phys. Rev. Lett. **69**, 1524 (1992).
[25] T. C. Jordan and M. T. Shaw, in *Proceedings of the Second International Conference on Electrorheological Fluids* [2], p. 231.
[26] C. M. Cerda, R. T. Foister, and S. G. Mason, J. Colloid Interface Sci. **82**, 577 (1981).
[27] T. C. Halsey and W. Toor, Phys. Rev. Lett. **65**, 2820 (1990); T. C. Halsey, in *Proceedings of the International Conference on Electrorheological Fluids: Mechanisms, Properties, Structures, Technology, and Applications* [3], p. 37; Science **258**, 761 (1992).
[28] K. C. Hass, Phys. Rev. E **47**, 3362 (1993).
[29] J. R. Melrose, in *Complex Fluids,* MRS Symposia Proceedings No. 248 (Materials Research Society, Pittsburgh, 1992), p. 275.
[30] D. J. Durian, D. A. Weitz, and D. J. Pine, J. Phys. Condens. Matter **2**, SA433 (1990); Science **252**, 686 (1991); Phys. Rev. A **44**, R7902 (1991).
[31] J. M. Ginder and L. D. Elie, in *Proceedings of the International Conference on Electrorheological Fluids: Mechanisms, Properties, Structure, Technology, and Applications* [3], p. 23.
[32] Advanced Fluid Systems Limited, London, England.
[33] The particle size quoted in a previous paper (Ref. [16]) was measured from a fractionated sample.
[34] See, e.g., B. J. Berne and R. Pecora, *Dynamic Light Scattering* (Wiley, New York, 1976).
[35] See, e.g., H. Z. Cummins and H. L. Swinney, Prog. Opt. **8**, 135 (1970).
[36] E. E. Uzgiris, Rev. Sci. Instrum. **45**, 74 (1974).
[37] B. Robertson, J. Chem. Phys. **95**, 3873 (1991).
[38] J. F. Miller, J. Colloid Interface Sci. **153**, 266 (1992).
[39] D. Brooks, J. Goodwin, C. Hjelm, L. Marshall, and C. Zukoski, Colloid Surf. **18**, 293 (1986).
[40] D. Stigter, J. Phys. Chem. **82**, 1417 (1978).
[41] See, e.g., R. E. Kornbrekke, I. D. Morrison, and T. Oja, Langmuir **8**, 1211 (1992).
[42] A. Ishimaru, *Wave Propagation and Scattering in Random Media* (Academic, New York, 1978), Vol. 1.
[43] G. Maret and P. E. Wolf, Z. Phys. B **65**, 409 (1987).
[44] D. J. Pine, D. A. Weitz, P. M. Chaikin, and E. Herbolzheimer, Phys. Rev. Lett. **60**, 1134 (1988); D. J. Pine, D. A. Weitz, J. X. Zhu, and E. Herbolzheimer, J. Phys. (Paris) **51**, 2101 (1990).
[45] S. Fraden and G. Maret, Phys. Rev. Lett. **65**, 512 (1990).
[46] X. L. Wu, D. J. Pine, P. M. Chaikin, J. S. Huang, and D. A. Weitz, J. Opt. Soc. Am. B **7**, 15 (1990).
[47] E. H. B. DeLacey and L. R. White, J. Chem. Soc. Faraday Trans. II **81**, 2007 (1981).
[48] W. C. Chew and P. N. Sen, J. Chem. Phys. **77**, 4683 (1982).
[49] H. Block, P. Rattray, and T. Watson, in *Proceedings of the International Conference on Electrorheological Fluids: Mechanisms, Properties, Structure, Technology, and Applications* [3], p. 93.
[50] *Scattering and Localization of Classical Waves,* edited by P. Sheng (World Scientific, Singapore, 1990).
[51] P. M. Morse and H. Feshbach, *Methods of Theoretical Physics* (McGraw-Hill, New York, 1953), Pts. I and II.
[52] I. Freund, Phys. Rev. A **45**, 8854 (1992), and references therein.
[53] See, e.g. A. Z. Genack, in *Scattering and Localization of Classical Waves* [50], p. 207.
[54] See, e.g., H. C. van de Hulst, *Light Scattering by Small Particles* (Dover, New York, 1981).
[55] P. M. Saulnier, M. P. Zinkin, and G. H. Watson, Phys. Rev. B **42**, R2621 (1990).
[56] J. B. Hayter and R. Pynn, Phys. Rev. Lett. **49**, 1103 (1983).
[57] M. Shapiro, A. L. Shalom, and I. J. Lin, J. Appl. Phys. **58**, 1028 (1985).
[58] T. Garino, D. Adolf, and B. Hance, in *Proceedings of the International Conference on Electrorheological Fluids: Mechanisms, Properties, Structure, Technology, and Applications* [3], p. 167.
[59] L. K. H. van Beek, in *Progress in Dielectrics,* edited by J. B. Birks (CRC Press, Cleveland, 1967), Vol. 7, p. 69.
[60] K. M. Baloch and T. G. M. van de Ven, J. Colloid Interface Sci. **129**, 91 (1989).
[61] See, e.g., W. B. Russel, D. A. Saville, and W. R. Schowalter, *Colloidal Dispersions* (Cambridge Univ. Press, Cambridge, 1989).
[62] F. C. MacKintosh and S. John, Phys. Rev. B **40**, 2383 (1989).
[63] See, e.g., G. K. Batchelor, J. Fluid Mech. **52**, 245 (1972).
[64] R. E. Cafflisch and J. H. C. Luke, Phys. Fluids **28**, 759 (1985).
[65] Z. Chen and P. Sheng, Phys. Rev. B **43**, 5735 (1991).
[66] D. J. Pine, D. A. Weitz, G. Maret, P. E. Wolf, E. Herbolzheimer, and P. M. Chaikin, in *Scattering and Localization of Classical Waves* [60], p. 312.

[67] A. Meller and J. Stavans, Phys. Rev. Lett. **68**, 3646 (1992).
[68] See, e.g., T. C. B. McLeish, T. Jordan, and M. T. Shaw, J. Rheol. **35**, 427 (1991).
[69] G. D. Scott and D. L. Mader, Nature (London) **201**, 382 (1964).
[70] G. P. Montgomery, Jr. and N. A. Vaz, Phys. Rev. A **40**, 6580 (1989).
[71] F. E. Filisko, in *Proceedings of the International Conference on Electrorheological Fluids: Mechanisms, Properties, Structure, Technology, and Applications* [3], p. 116.
[72] A. J. Hurd, S. Fraden, and R. B. Meyer, in *Science of Ceramic Chemical Processing,* edited by L. L. Hench and D. R. Ulrich (Wiley, New York, 1986), p. 555.
[73] D. L. Klass and T. W. Martinek, J. Appl. Phys. **38**, 67 (1967).